The relationship of grey and white matter abnormalities with distance from the surface of the brain in multiple sclerosis

Matteo Pardini[1,2], Carole H. Sudre[3,4], Ferran Prados[1,3], Özgür Yaldizli[1,5], Varun Sethi[1], Nils Muhlert[1,6,7], Rebecca S. Samson[1], Steven H. van de Pavert[1], M. Jorge Cardoso[3,4], Sebastien Ourselin[3,4], Claudia AM Gandini Wheeler-Kingshott[1,8,9], David H. Miller[1,10], and Declan T. Chard[1,10].

Affiliations:

1. Queen Square MS Centre, NMR Research Unit, Department of Neuroinflammation, UCL Institute of Neurology, London, UK
2. Department of Neuroscience, Rehabilitation, Ophthalmology, Genetics, Maternal and Child Health, University of Genoa and IRCCS AOU San Martino-IST, Genoa, Italy.
3. Translational Imaging Group, Centre for Medical Image Computing (CMIC), Department of Medical Physics and Bioengineering, University College London, London, UK
4. Dementia Research Centre, UCL Institute of Neurology, London, UK
5. Department of Neurology, University Hospital Basel, Basel, Switzerland
6. School of Psychology and Cardiff University Brain Research Imaging Centre, Cardiff University, Cardiff, UK
7. School of Psychological Sciences, University of Manchester, Manchester UK
8. Brain MRI 3T Center, C. Mondino National Neurological Institute, Pavia, Italy.
9. Department of Brain and Behavioural Sciences, University of Pavia, Pavia, Italy
10. National Institute for Health Research (NIHR) University College London Hospitals (UCLH) Biomedical Research Centre, UK

Manuscript information: Title (characters): 120. N. words in the abstract: 244. N. words in the main text: 2604. Figures: 4. Tables: 2. References: 32. Supplementary Tables: 1

Correspondence to: Dr. Declan Chard, Queen Square Multiple Sclerosis Centre, UCL Institute of Neurology, Queen Square, London WC1N 3BG London Email: d.chard@ucl.ac.uk

Abstract

Objective: To assess the association between proximity to the inner (ventricular and aqueductal) and outer (pial) surfaces of the brain and the distribution of normal appearing white matter (NAWM) and grey matter (GM) abnormalities, and white matter (WM) lesions, in multiple sclerosis (MS).

Methods: 67 people with relapse-onset MS and 30 healthy controls were included in the study. Volumetric T1 images and high-resolution (1 mm^3) magnetization transfer ratio (MTR) images were acquired and segmented into 12 bands between the inner and outer surfaces of the brain. The first and last bands were discarded to limit partial volume effects with cerebrospinal fluid. MTR values computed for all bands in supra-tentorial NAWM, cerebellar NAWM and brainstem NA tissue, and deep and cortical GM. Band WM lesion volumes were also measured.

Results: Proximity to the ventricular surfaces was associated with progressively lower MTR values in the MS group but not in controls in in supra-tentorial and cerebellar NAWM, brainstem NA and in deep and cortical GM. The density of WM lesions was associated with proximity to the ventricles only in the supra-tentorial compartment, and no link was found with distance from the pial surfaces.

Conclusions: In MS MTR abnormalities in NAWM and GM are related to distance from the inner and outer surfaces of the brain, and this suggests that there is a common factor underling their spatial distribution. A similar pattern was not found for WM lesions, raising the possibility that different factors promote their formation.

Keywords: multiple sclerosis, normal appearing tissue, magnetisation transfer ratio.

Introduction

Multiple sclerosis (MS) can affect any part of the central nervous system, but it does not do so uniformly. Histopathological studies have shown that demyelinating lesions in white matter (WM) and grey matter (GM) tend to occur close to the inner (periventricular) and outer (subpial) surfaces of the brain[1,2] and that, at least in GM, extra-lesional abnormalities are also greater near the surfaces of the brain.[1,3] Using magnetisation transfer ratio (MTR) imaging, similar gradients in cortical GM abnormalities have been shown *in vivo*[4], and have also been found in periventricular WM[5] and the spinal cord.[6] Taken together, these observations suggest that tissues close to the surface of the brain and spinal cord are preferentially affected by, or more vulnerable to the effects of, MS.

Several explanations for the distribution of MS lesions have been proposed. Veins have been firmly implicated, and WM lesions nearly always form around them.[7-9] Many GM lesions also do so,[10] although subpial cortical GM lesions do not appear to and instead have been linked with overlying meningeal inflammation.[11-12] The same factors underlying the distribution of lesions may also be relevant for extra-lesional pathology, but this has been studied far less. In GM, meningeal inflammation has been linked with both subpial lesions and extra-lesional cortical GM neuronal loss[1] but we are not aware of equivalent studies systematically investigating WM.

While there are several potential mechanisms that may underly MS lesional and extra-lesional abnormalities, and pathology in GM and WM, it is not clear if a single process unites them. Two key unanswered questions that are relevant to this: (1) Are superficial gradients in MS abnormalities similar in WM and GM; and (2) are they similar for WM lesions and extra-lesional abnormalities? To answer these questions we systematically assessed MS-associated reductions in GM and WM MTR, and the distribution of WM lesions, relative to the inner and outer surfaces of the brain.

Methods

Participants

People with a relapse onset MS,[13] and healthy controls (HC), with no known neurological disease, between 18 and 65 years old, were recruited for this study. Data from 67 people with MS (20 males/47 females; mean age: 45.12±1.02 years; median EDSS: 4 [range 1-8]; 41 with relapsing remitting MS and 26 with secondary progressive MS) and 30 HCs (15 males/15 females; mean: 41.03±2.01 years) was obtained. All participants gave written informed consent. This study was approved by our local institutional ethics committee.

MRI acquisition

Using a 3 T Philips Achieva system (Philips Healthcare) with a 32-channel head coil and multi-transmit technology, the following sequences were acquired: 3D sagittal T1-weighted fast field echo (FFE) scan: 1 x 1 x 1 mm^3, inversion time = 824 ms, repetition time = 6.9 ms, echo time = 3.1 ms; dual-echo proton density/T2-weighted axial-oblique scans aligned with the anterior to posterior commissure line (1 x 1 x 3 mm^3, repetition time = 3500 ms, echo time = 19/85 ms); and high resolution magnetization transfer imaging using a 3D slab-selective FFE sequence with two echoes: 1 x 1 x 1 mm^3, repetition time = 6.4 ms, echo time = 2.7/4.3 ms, alpha = 9° with and without sinc Gaussian-shaped magnetization transfer pulses of nominal alpha = 360°, offset frequency 1 kHz, duration 16 ms. A turbo field echo (TFE) readout was used, with an echo train length of four, TFE shot interval 32.5 ms, giving a total time between successive magnetization transfer pulses of 50 ms, and scan time of 25 min. The two echoes were averaged (thereby increasing the signal-to-noise ratio) for both the magnetization transfer on and off data.

Image analysis

Registration of images

The magnetisation transfer on and off images were symmetric- and inverse-consistent registered to the T1-weighted FFE scan using NiftyReg.[14-15] MTR map (in percentage units (pu)) was calculated as ((MTRoff – MTRon) / MToff) x 100).

WM lesions identification

WM lesions were identified and manually outlined on PD/T2-weighted scans using JIM (Version 6.0, Xinapse Systems, Northants) by OY and VS, and rechecked by DC.

Lesion filling

The PD/T2-weighted lesion masks were affine co-registered to the T1-weighted FFE scans using a pseudo-T1 image generated by subtracting the PD from the T2-weighted image.[16] Lesion masks were transformed from native space to T1 space using nearest-neighbour interpolation. The T1-weighted FFE scans were filled using a non-local patch match lesion filling technique.[17]

Brain segmentation

For brain tissue segmentation, we used Geodesical Information Flows (GIF).[18] GIF is a segmentation technique that uses imaging databases as sources of information and is able to propagate voxel-wise annotations, such as tissue segmentation or parcellation, between morphologically dissimilar images by diffusing and mapping the available examples through intermediate steps. GIF is part of NiftySeg (http://niftyseg.sf.net) software package and is free available as online tool at NiftyWeb[19] (http://cmictig.cs.ucl.ac.uk/niftyweb). The image database used for this study is labeled according to the Neuromorphometrics protocol (http://www.neuromorphometrics.com/). T1-weighted volumetric images were segmented into whole brain GM, WM and cerebrospinal fluid (CSF). These images were used to calculate Brain parenchymal fraction (BPF) as: (GM volume + WM volume) / (GM volume + WM volume + CSF volume). GIF was also used to create the cortical GM, subcortical GM, supra-tentorial WM, cerebellar WM, and brainstem parcellation masks.

Extraction of normal appearing white matter

As in our previous work,[5] to reduce the potential for lesional and peri-lesional abnormalities contaminating the normal appearing (NA) WM measures, lesions and a 2 mm peri-lesional rim were subtracted from each subject's WM mask to produce a NAWM mask. Moreover, as the brainstem includes both white matter and grey nuclei, lesions were and the 2 mm peri-lesional rim were also removed from the brainstem mask parcellation mask to produce a brainstem normal appearing tissue (NAT) mask.

Bands computation

The whole brain was segmented into 12 concentric bands between the ventricular walls and the pial surfaces (Figure 1) based on the normalized distance map derived by following the normal to the Laplace equation isolines between the subpial and periventricular brain surfaces.[4,20,21] The first and last band, i.e. those nearest to the ventricular and pial surfaces, were then excluded from further analysis to control for CSF partial volume effects, so leaving 10 bands, with bands 1 and 10 located adjacent to periventricular and subpial surfaces respectively. Average volume for each band is reported in Supplemental Table 1. We defined the bands 1-3 as encompassing the periventricular , bands 4-7 the central and bands 8-10 the subpial region. The bands were then intersected with the cortical (supra-tentorial and cerebellar) and deep GM (thalamus, caudate and putamen nuclei), supra-tentorial and cerebellar NAWM, and brainstem NAT masks to extract mean MTR. Lesion volumes were measured in WM, and the mean percentage occupied by lesions computed for each band.

Quantification of gradients and of lesion volumes

The following gradients were then computed for each subject

- Periventricular gradient: The periventricular gradient was quantified as (MTR in band 3 – MTR in band 1) / 2. It was computed separately for supra-tentorial NAWM and cerebellar NAWM, brainstem NAT and for deep GM.

- Central gradient: The central gradient was quantified as: (MTR in band 7 – MTR in band 4) / 3. It was computed separately for supra-tentorial NAWM and cerebellar NAWM, brainstem NAT and for deep GM.

- Subpial gradient: The subpial gradient was quantified as (MTR in band 10 – MTR in band 8) / 2. It was computed separately in the brainstem NAT as well as in cortical GM.

Lastly, the percentage of lesional WM was quantified in periventricular (bands 1 to 3), deep (bands 4 to 7) and subpial (bands 8 to 10) regions as: 100 x WM band lesion volume / WM band volume.

Statistical analysis

MRI measures were compared between MS and HC subjects using a general linear model including BPF, age, gender and band volume as covariates. A false discovery rate (FDR) approach as described by Benjamini and Hochberg was used to control for multiple comparisons.[22] In all the analyses a p-value < 0.05 was considered statistically significant.

Results

MTR abnormalities with proximity to the ventricular surfaces

Supra-tentorial and cerebellar NAWM and brainstem NAT MTR findings for the MS and HC groups are shown in Figure 2, and Tables 1 and 2. In the supra-tentorial NAWM, cerebellar NAWM and brainstem NAT, MS subjects had lower MTR values compared with HC. This reduction in MTR was more marked in those bands nearer to the ventricular surfaces, and a steeper periventricular MTR gradient was observed in MS subjects when compared with HC in all these compartments (Table 1; supra-tentorial: $p=0.003$, cerebellar: $p=0.012$, brainstem: $p=0.015$; p values corrected for BPF, age, gender and band volume). A significant difference between the periventricular and central gradients was also observed in MS subjects ($p<0.001$ for all compartments).

Deep GM MTR findings are shown in Figure 3, and Table 1. An MS-associated reduction in deep GM MTR increased with proximity to the ventricular surface, and a steeper periventricular MTR gradient was observed in MS subjects compared with HC (Table 1; $p=0.025$; ; p value corrected for BPF, age, gender and band volume). A significant difference between periventricular and central gradient was observed in the MS group ($p<0.001$).

.

MTR abnormalities with proximity to the pial surfaces

In subpial NAT bands in the brainstem (bands 8-10) MTR was lower in MS compared with the HC group, as reported in Table 2. This reduction was more marked in those bands nearest to the subpial surface (Figure 2), and a steeper subpial MTR gradient was observed in MS subjects compared to HC ($p=0.015$; p value corrected for BPF, age, gender and band volume). A significant difference between subpial and central gradients also observed in MS group ($p<0.001$).

Cortical GM MTR results are shown in Figure 4 and Table 2. The cortical GM subpial gradient was significantly steeper in subjects with MS compared with HC (p=0.020; p value corrected for BPF, age, gender and band volume).

Lesion density and proximity to brain surfaces

The density of WM lesions per band is shown in Figure 3. In the supra-tentorial compartment, lesion density was highest around the ventricles and decreased towards central WM (5.80%±0.70 vs 2.50%±0.40, p=0.005**;** p value corrected for BPF, age, gender and band volume). In the cerebellum and brainstem there was no association between proximity to the fourth ventricle and WM lesion density.

Discussion

We found that MS-associated reductions in supra-tentorial and cerebellar NAWM, brainstem NAT, and cortical and deep GM MTR are related to distance from the inner (ventricular) and outer (pial) surfaces throughout the brain. In contrast, for WM lesions a relationship with distance from the brain surface was only seen around the lateral ventricles. This suggests that proximity to the surface of the brain *per se* may be relevant to the pathogenesis of NAWM and GM abnormalities, but is less important for the accrual of WM lesions, and so raises the possibility that partly independent processes may underlie them.

We have previously found associations between cortical GM MTR and distance from the outer surface of the brain[4], and NAWM MTR and proximity to the lateral ventricles.[5] The present results confirm these findings, and also show that these superficial gradients in MTR abnormalities are consistent throughout the brain. In agreement with previous lesion probability studies,[23] we found that WM lesion density was highest around the lateral ventricles. However, no gradient in WM lesion density was seen with distance from the fourth ventricle in the brainstem or cerebellum, which clearly contrasts with the MTR findings in NAWM and GM in these regions. While it is possible that the same factors underlie the gradients in MTR abnormalities and the distribution of WM lesions, the discrepancy between them does raise the distinct possibility that different processes are at work.

WM lesions mostly form around veins,[7-8] and our results would appear consistent with this. Around the lateral ventricles, where a gradient in lesion density was seen, veins drain towards the periventricular ependymal surface. In contrast, in the brainstem and cerebellum, where a gradient in lesion density was not seen, venous drainage is not so uniformly towards the fourth ventricle.[24-25]

The consistency of superficial gradients in MTR abnormalities throughout brain GM and NAWM is difficult to explain based on the distribution of veins, or hypoxia, given substantial differences in vascular architecture and perfusion between brain regions.[24-26] A CSF-mediated factor perhaps offers a more straightforward explanation, being in

close proximity to both the inner and outer brain surfaces. However, while there is *in vitro* evidence that CSF from people with MS is both myelo- and neurotoxic,[27,28] this has not been shown *in vivo.* Meningeal inflammation has been implicated in the pathogenesis of cortical GM lesions, and lesional and extra-lesional neuronal loss,[11-12] but ependymal changes in MS do not appear to be closely linked with underlying WM lesion formation[1] and, to the best of our knowledge, no studies have looked for associations between ependymal abnormalities and axonal pathology in WM.

Our study also confirms previous findings that have shown that - even in HC - MTR is not uniform throughout WM.[29] In this study we found that MTR values in supratentorial WM were highest adjacent to the ventricles, declining with distance from them, and particularly next to the cortex. In WM MTR has previously been shown to be sensitive to both myelin and axonal densities[30] and so the regional MTR patterns we have observed may stem from differences in myelin and axonal organisation. We are not aware of any histopathological studies that have specifically addressed this, and as such cannot speculate further. Practically, this finding highlights the need to take into account regional differences in MTR when evaluating the impact of disease processes on WM.

While carefully designed, the methods used in this study still have limitations. To reduce the potential for partial volume effects a GIF-based segmentation approach was used, which explicitly models partial volumes. Moreover, the bands nearest to the inner and outer brain surfaces were excluded from the analyses, so further reducing the possible impact of CSF contamination. While all registrations were carefully checked, brain atrophy could still have subtly affected the relative positioning of bands between subjects, and so reduced sensitivity to MTR gradients. However, the Laplace-based approach used in this study will have partially accounted for the differences in brain size as the number of bands extracted for each subject was the same, and so while in people with greater atrophy each band will be narrower, their position relative to the surface of the brain should be maintained. As in our previous study on NAWM,[5] we dilated WM lesion masks by 2mm to allow for perilesional disease effects.[31] This, together with the observed differences in the distribution of NAWM MTR abnormalities and WM lesions makes unlikely that contamination of NAWM by lesions will have

significantly influenced the results. However, while most WM lesions are seen on PD/T2-weighted scans, few GM lesions are detected using currently available MRI techniques,[32] and as such it is not possible for us to determine if the abnormal MTR gradient observed in GM is due to lesional or extra-lesional pathology. Histopathological studies of the cortex[1] and in deep GM[3] suggests that it may be due to both. While this does not negate the main findings of our work, it is an area that could usefully be clarified in subsequent studies.

In conclusion, abnormalities in NAWM and GM (as assessed using MTR) are both associated with proximity to the inner and outer surfaces of the brain, raising the possibility of a common pathogenic factor underlying them. In contrast, while WM lesions preferentially accrue around the lateral ventricles, their distribution elsewhere is not consistently related to distance from the surface of the brain, suggesting the possibility that different factors may promote their formation.

References

1. Magliozzi R, Howell OW, Reeves C, et al. A Gradient of neuronal loss and meningeal inflammation in multiple sclerosis. Ann Neurol 2010;**68**:477–93.

2. Brownell B, Hughes JT. The distribution of plaques in the cerebrum in multiple sclerosis. J Neurol Neurosurg Psychiatry 1962; **25**: 315-20

3. Vercellino M, Masera S, Lorenzatti M, et al. Demyelination, inflammation, and neurodegeneration in multiple sclerosis deep gray matter. J Neuropathol Exp Neurol 2009;**68**:489–502.

4. Samson RS, Cardoso MJ, Muhlert N, et al. Investigation of outer cortical magnetisation transfer ratio abnormalities in multiple sclerosis clinical subgroups. Mult Scler 2014;**20**:1322–30.

5. Liu Z, Pardini M, Yaldizli O, et al. Magnetization transfer ratio measures in normal-appearing white matter show periventricular gradient abnormalities in multiple sclerosis. Brain 2015;**138**:1239–46

6. Kearney H, Yiannakas MC, Samson RS, et al. Investigation of magnetization transfer ratio-derived pial and subpial abnormalities in the multiple sclerosis spinal cord. Brain 2014;**137**:2456–68.

7. Adams CW, Abdulla YH, Torres EM, et al. Periventricular lesions in multiple sclerosis: their perivenous origin and relationship to granular ependymitis. Neuropathol Appl Neurobiol 1987;**13**:141–52.

8. Mistry N, Dixon J, Tallantyre E, et al. Central veins in brain lesions visualized with high-field magnetic resonance imaging: a pathologically specific diagnostic biomarker for inflammatory demyelination in the brain. JAMA Neurol 2013;**70**:623–8.

9. Haider L, Zrzavy T, Hametner S, et al. The topograpy of demyelination and neurodegeneration in the multiple sclerosis brain. Brain 2016; **139**:807-15.

10. Kidd D, Barkhof F, McConnell R, et al. Cortical lesions in multiple sclerosis. Brain 1999;122:17–26.

11. Magliozzi R, Howell O, Vora A, et al. Meningeal B-cell follicles in secondary progressive multiple sclerosis associate with early onset of disease and severe cortical pathology. Brain 2007;**130**:1089–104.

12. Howell OW, Reeves CA, Nicholas R, et al. Meningeal inflammation is widespread and linked to cortical pathology in multiple sclerosis. Brain 2011;**134**:2755–71.

13. Polman CH, Reingold SC, Edan G, et al. Diagnostic criteria for multiple sclerosis: 2005 Revisions to the 'McDonald Criteria'. Ann. Neurol. 2005;**58**:840–6.

14. Modat M, Cash DM, Daga P, et al. Global image registration using a symmetric block-matching approach. J Med imaging (Bellingham, Wash) 2014;**1**:024003.

15. Modat M, Ridgway GR, Taylor ZA, et al. Fast free-form deformation using graphics processing units. Comput Methods Programs Biomed 2010;**98**:278–84.

16. Hickman S, Barker G, Molyneux P, et al. Technical note: the comparison of hypointense lesions from 'pseudo-T1' and T1-weighted images in secondary progressive multiple sclerosis. Mult Scler 2002;**8**:433–5.

17. Prados F, Cardoso MJ, MacManus D, et al. A modality-agnostic patch-based technique for lesion filling in multiple sclerosis. In: Lecture Notes in Computer Science). Springer Verlag 2014;781–8.

18. Cardoso MJ, Modat M, Wolz R, et al. Geodesic Information Flows: Spatially-Variant Graphs and Their Application to Segmentation and Fusion. IEEE Trans Med Imaging 2015;**34**:1976–88.

19. Prados F, Cardoso MJ, Burgos N, et al. NiftyWeb: web based platform for image processing on the cloud. International Society for Magnetic Resonance in Medicine (ISMRM) 24th Scientific Meeting and Exhibition - Singapore 2016

20. Cardoso MJ, Clarkson MJ, Ridgway GR, et al. LoAd: A locally adaptive cortical segmentation algorithm. Neuroimage 2011;**56**:1386–97.

21. Yezzi AJ, Prince JL. An Eulerian PDE Approach for Computing Tissue Thickness. IEEE Trans Med Imaging 2003;**22**:1332–9.

22. Benjamini Y, Hochberg Y. Controlling the False Discovery Rate: A practical and powerful approach to multiple testing. J R Stat Soc Series B Stat Methodol. 1995; **57**: 289–300.

23. Lee MA, Smith S, Palace J, et al. Spatial mapping of T2 and gadolinium-enhancing T1 lesion volumes in multiple sclerosis: Evidence for distinct mechanisms of lesion genesis? Brain 1999;**122**:1261–70.

24. Wang J, Wang J, Sun J, et al. Evaluation of the anatomy and variants of internal cerebral veins with phase-sensitive MR imaging. Surg. Radiol. Anat. 2010;**7**:1–6.

25. Duvernoy HM. The superficial veins of the human brain — Veins of the brain stem and of the base of the brain. Berlin: Springer-Verlag. 1975.

26. Watabe T, Shimosegawa E, Kato H, et al. CBF/CBV maps in normal volunteers studied with 15O PET: a possible index of cerebral perfusion pressure. Neurosci Bull 2014;**5**:857–62.

27. Ménard A, Pierig R, Pelletier J, et al. Detection of a gliotoxic activity in the cerebrospinal fluid from multiple sclerosis patients. Neurosci Lett 1998;**245**:49–52.

28. Vidaurre OG, Haines JD, Katz Sand I, et al. Cerebrospinal fluid ceramides from patients with multiple sclerosis impair neuronal bioenergetics. Brain 2014;**137**:2271–86.

29. Mehta RC, Pike GB, Enzmann DR.Magnetization transfer MR of the normal adult brain. AJNR Am J Neuroradiol. 1995; **16**:2085-91.

30. Schmierer K, Scaravilli F, Altmann DR, Barker GJ, Miller DH. Magnetization transfer ratio and myelin in postmortem multiple sclerosis brain. Ann Neurol. 2004;**56**:407-15.

31. Vrenken H, Geurts JJG, Knol DL, et al. Normal-appearing white matter changes vary with distance to lesions in multiple sclerosis. Am J Neuroradiol 2006;**27**:2005–11.

32. Geurts JJG, Bö L, Pouwels PJW, et al. Cortical lesions in multiple sclerosis: Combined postmortem MR imaging and histopathology. Am J Neuroradiol 2005;**26:**572–7.

Disclosures

Dr. Pardini received research support from Novartis.
Ms. Sudre reports no disclosure.
Dr. Prados reports no disclosures.
Dr. Yaldizli has received lecture fees from Teva, Novartis and Bayer Schering which was exclusively used for funding of research and continuous medical education in the Department of Neurology at the University Hospital Basel.
Dr. Sethi receives research support from Biogen Idec and Novartis.
Dr. Muhlert reports no disclosures.
Dr. Samson reports no disclosures.
Mr. van de Pavert reports no disclosures.
Dr. Cardoso reports no disclosures
Prof. Ourselin reports no disclosures
Prof. Wheeler-Kingshott is on the advisory board for BG12 (Biogen).
Prof. Miller has received honoraria from Biogen Idec, Novartis, GlaxoSmithKline, and Bayer Schering, and research grant support for doing MRI analysis in multiple sclerosis trials sponsored by GlaxoSmithKline, Biogen Idec, and Novartis.
Dr. Chard has received honoraria (paid to his employer) from Ismar Healthcare NV, Swiss MS Society, Excemed (previously Serono Symposia International Foundation), Merck, Bayer and Teva for faculty-led education work; Teva for advisory board work; meeting expenses from Merck, Teva, Novartis, the MS Trust and National MS Society; and has previously held stock in GlaxoSmithKline.

Acknowledgements

FP is funded by the National Institute for Health Research University College London Hospitals Biomedical Research Centre (NIHR BRC UCLH/UCL High Impact Initiative). SO is funded by the Engineering and Physical Sciences Research Council (EP/H046410/1, EP/J020990/1, EP/K005278), the Medical Research Council (MR/J01107X/1), the EU-FP7 project VPH-DARE@IT (FP7- ICT-2011-9-601055), and the National Institute for Health Research University College London Hospitals Biomedical Research Centre (NIHR BRC UCLH/UCL High Impact Initiative

BW.mn.BRC10269). Declan Chard has received research support from the MS Society of Great Britain and Northern Ireland, and the National Institute for Health Research University College London Hospitals Biomedical Research Centre.

Founding statement

The NMR Research Unit is supported by the UCLH Comprehensive Biomedical Research Centre and the MS Society of Great Britain and Northern Ireland, which provided support for the study.

Contribution statements

Matteo Pardini Study concept and design, analysis & interpretation of data, drafting of manuscript, statistical analysis
Carole H. Sudre: Analysis & interpretation of data critical revision of manuscript
Ferran Prados Analysis & interpretation of data critical revision of manuscript
Özgür Yaldizli Analysis & interpretation of data critical revision of manuscript
Varun Sethi: Acquisition of data, Analysis & interpretation of data critical revision of manuscript
Nils Muhlert: Acquisition of data, critical revision of manuscript
Rebecca S. Samson: Analysis & interpretation of data, critical revision of manuscript, technical support.
Steven H. van de Pavert: Analysis & interpretation of data critical revision of manuscript
M. Jorge Cardoso: interpretation of data, critical revision of manuscript, study supervision
Sebastien Ourselin: interpretation of data, critical revision of manuscript, study supervision
Claudia AM Gandini Wheeler-Kingshott: MRI protocol setup, critical revision of manuscript, technical support, study supervision.
David H. Miller: Study concept and design, interpretation of data, critical revision of manuscript, study supervision
Declan T. Chard Study concept and design, analysis & interpretation of data, critical revision of manuscript, study supervision.

Figure legends

Figure 1. Brain parenchyma segmentation in twelve bands based on the iterative application of the normalised central curve of the Laplace equation. Each band is represented by a different colour.

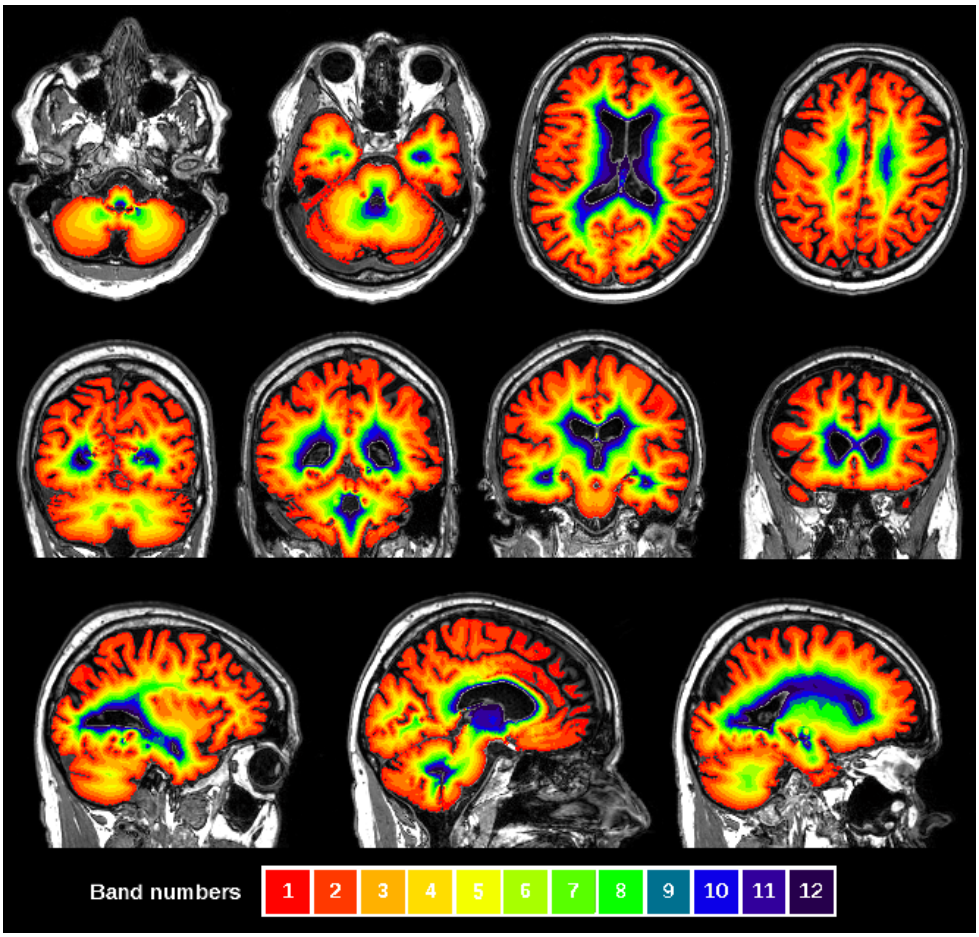

Figure 2. Supra-tentorial and cerebellar normal appearing white matter (NAWM) and brainstem NA tissue (NAT) data. MTR values for MS subjects (red dots) and controls (blue dots). Error bars represent 2 x standard errors (SE). Bands 1-3 represent the periventricular region (with band 1 nearest to the ventricular surface), bands 4-7 the central region and bands 8-10 the subpial region (with band 10 nearest to the pial surface).

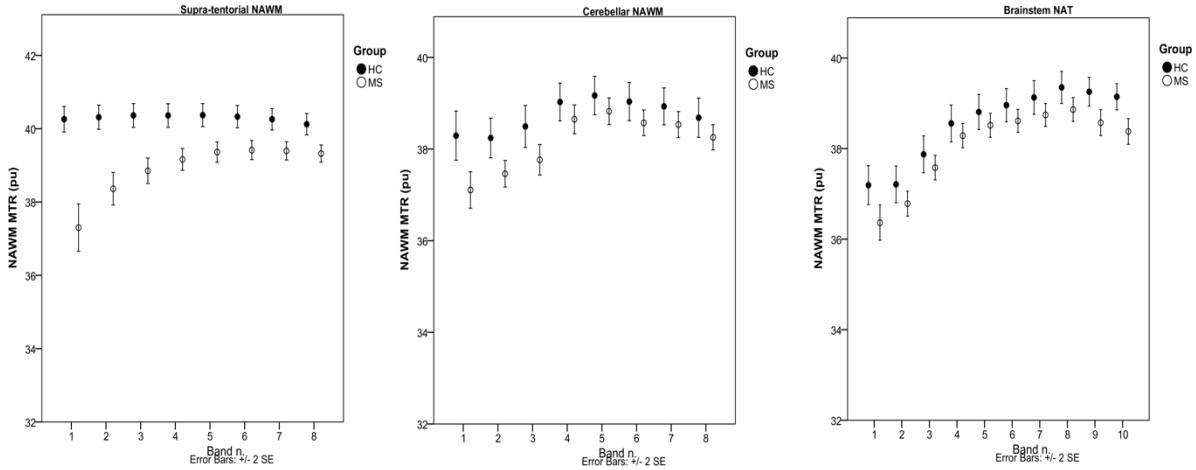

Figure 3. Grey matter (GM) data MTR values for MS subjects (red dots) and controls (blue dots). Error bars represent 2 x standard errors (SE). Bands 1-3 represent the periventricular region (with band 1 nearest to the ventricular surface), bands 4-7 the central region and bands 8-10 the subpial region (with band 10 nearest to the pial surface).

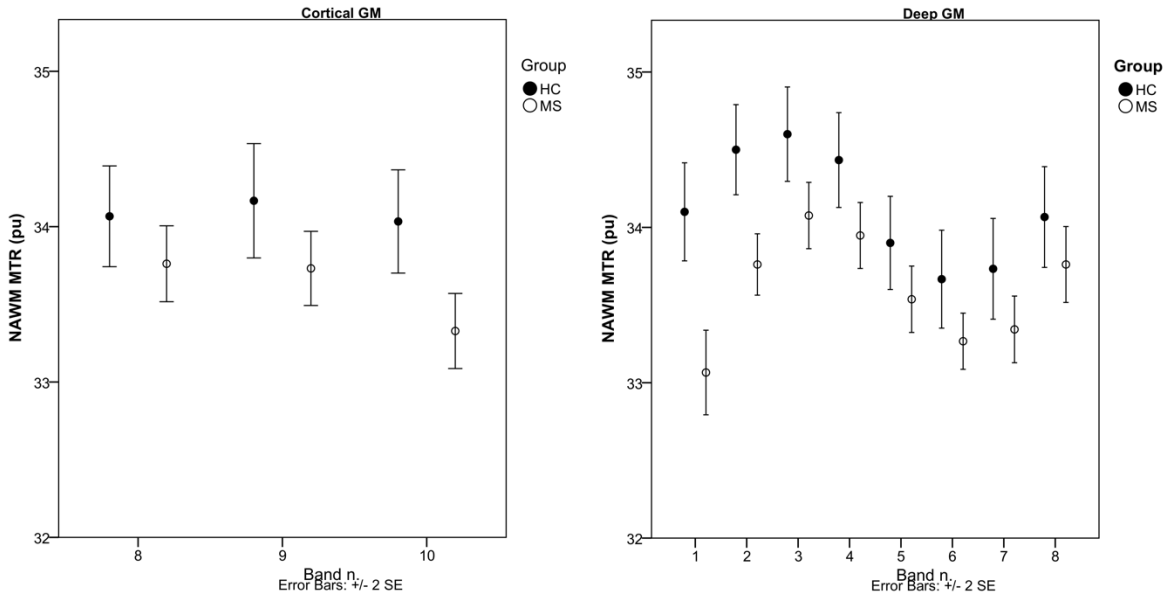

Figure 4. Percentage of lesioned white matter (WM) for each band in the supra-tentorial, cerebellar and brainstem white matter in the MS group. Error bars represent 2 x standard errors (SE). Band 1 is the nearest to the ventricular surface, band 10 is the nearest to the pial surface.

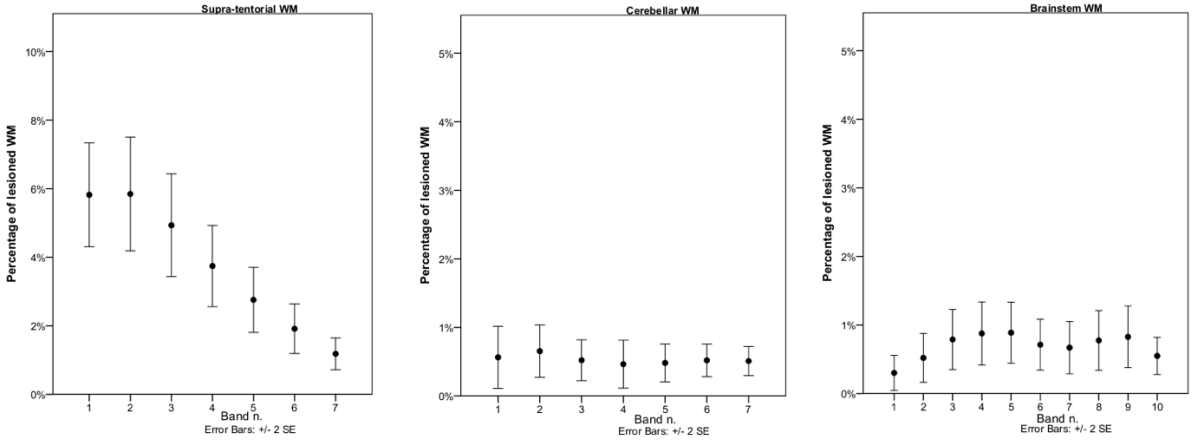

Table 1. MRI measures in the periventricular and central regions. *P-values* are computed using a general linear model including BPF, age, gender and band volume as covariates. Those values surviving a threshold of 0.05 FDR-corrected for multiple comparisons are marked in bold font and underlined. Legend: NAWM: normal appearing white matter, NAT: normal appearing tissue. GM: grey matter, MS: multiple sclerosis subjects, HC: healthy controls, MTR: magnetisation transfer ratio.

Region	**Measure**	**MTR**		
		HC	**MS**	**Difference**
Supra-tentorial NAWM	Band 1	40.26±0.17	37.20±0.32	**p<0.001**
	Band 3	40.36±0.16	38.85±0.17	**p<0.001**
	Band 4	40.35±0.15	39.16±0.15	**p<0.001**
	Band 7	40.20±0.16	39.39±0.20	**p=0.001**
	Periventricular gradient	0.05±0.16	0.85±0.17	**p=0.003**
	Central gradient	0.00±0.08	-0.02±0.09	p=0.820
Cerebellar NAWM	Band 1	38.29±0.26	37.11±0.19	**p=0.008**
	Band 3	38.49±0.22	37.77±0.14	**p=0.012**
	Band 4	39.03±0.20	38.65±0.16	p=0.210
	Band 7	38.93±0.20	38.53±0.15	**p=0.025**
	Periventricular gradient	0.10±0.04	0.33±0.05	**p=0.012**
	Central gradient	-0.03±0.05	-0.03±0.06	p=0.800

Brainstem NAT	Band 1	37.19±0.21	36.36±0.20	**p=0.010**
	Band 3	37.87±0.20	37.58±0.14	p=0.285
	Band 4	38.56±0.20	38.28±0.13	p=0.310
	Band 7	39.13±0.18	38.73±0.13	p=0.138
	Periventricular gradient	0.34±0.05	0.61±0.06	**p=0.015**
	Central gradient	0.19±0.02	0.15±0.02	p=0.190
Deep GM	Band 1	34.10±0.15	33.07±0.14	**p=0.005**
	Band 3	34.60±0.15	34.08±0.15	**p=0.012**
	Band 4	34.43±0.14	39.16±0.15	**p=0.020**
	Band 7	33.73±0.16	33.34±0.11	p=0.050
	Periventricular gradient	0.25±0.05	0.50±0.06	**p=0.025**
	Central gradient	0.00±0.10	0.08±0.08	p=0.635

Table 2. MRI measures in the subpial regions. P-values are computed using a general linear model including BPF, age, gender and band volume as covariates. Those values surviving a threshold of 0.05 FDR-corrected for multiple comparisons are marked in bold font and underlined. Legend: NAWM: normal appearing white matter, NAT: normal appearing tissue, GM: grey matter, MS: multiple sclerosis subjects, HC: healthy controls, MTR: magnetisation transfer ratio.

Region	**Measure**	**MTR**		
		HC	**MS**	**Differences**
Brainstem NAT	Band 8	39.35±0.17	38.86±0.13	p=0.049
	Band 10	39.14±0.14	38.38±0.14	**p=0.010**
	Subpial gradient	-0.10±0.05	-0.24±0.02	**p=0.015**
Cortical GM	Band 8	34.07±0.16	33.76±0.12	p=0.158
	Band 10	34.03±0.16	33.33±0.12	**p=0.020**
	Subpial gradient	-0.01±0.02	-0.14±0.02	**p=0.020**

Supplementary Table 1. Average volume in cubic millimiters for each band. Legend: MS: multiple sclerosis, HC: Healthy controls

Band N.	HC	MS
1	17845±352	17421±382
2	22133±513	20680±324
3	25641±586	27534±439
4	34004±690	30740±352
5	41889±817	37705±534
6	51937±993	46662±656
7	65736±1259	59189±820
8	86894±1647	78564±1050
9	124007±2211	112559±1428
10	199003±3296	180509±2250